

## Supporting information

Catalysis of gamma-valerolactone conversion by zinc doping microporous materials

Catalyst preparation:

### 1. AlPO-5 and Zn-AlPO-5

The synthesis of AlPO-5 started with the process described: Slowly added 5.1g of aluminium isopropoxide (Acros, 98%) into a solution mixed by 2.88g of 85% phosphoric acid (Aldrich, 99%) and 10g of deionised water. After agitation for 24 hours, 2.52g of trimethylamine (Fisher scientific) was added to the gel. The pH value for the final gel was approximately 10. After another 1 hour of agitation, the gel was transferred to a Teflon liner in an autoclave. The autoclave was heated in an oven at 180°C for 72 hours. After crystallisation, the sample was cooled down to room temperature and washed by deionised water. The final product was obtained after drying at 100°C in an oven overnight followed by calcination in air at 550°C for 12 hours with the ramp rate of 5°C/min. The synthesis method of substituted Zn-AlPO-5 was similar to AlPO-5, however, the organic template was 3.9g of N,N-Dicyclohexylmethylamine (Aldrich, 97%) instead of trimethylamine. In addition, another 0.27g of zinc acetate dehydrate (Sigma-Aldrich, 99%) was added to the gel and the amount of aluminium isopropoxide reduced by 0.25g. The pH value of the precursor gel for Zn-AlPO-5 was approximate 6.

### 2. ZSM-5 and Zn-ZSM-5

ZSM-5 was provided by Sinopec, China. According to inductively coupled plasma-atomic emission spectroscopy (P-4010/ICP-AES), the Si/Al ratio in this material was 19.25. Before using the sample it was calcined in air at 480°C for 2 hours with a ramp rate of 1°C/min. In terms of the preparation of ion exchanged Zn-ZSM-5, 2g of unmodified ZSM-5 was soaked in a 30ml zinc nitrate solution composed of 10.32g of zinc nitrate hexahydrate (Sigma-Aldrich, 98%) and 30ml deionised water. After agitation at room temperature in a round bottom flask for 24 hours, the sample was washed with deionised water and subsequently dried at 100°C overnight. Finally, the powder was calcined in air at 550°C for 12 hours with a ramp rate of 5°C/min.

Catalytic evaluation

### 1. Reactor

The catalytic reaction took place in a HEL fix bed reactor. Figure S1 was the configuration of the reactor. A 2 hours pre-treatment under 400 °C with ramp rate of 10 °C per minute was performed for all catalysts. During the reaction, a 40wt% GVL/water solution with flow rate 0.016ml/min was pumped into a fixed bed stainless steel reactor that hosted the catalysts sandwiched by quartz wool plugs. The carrier gas was N<sub>2</sub> with a feed rate of 3 cm<sup>3</sup> min<sup>-1</sup> at reaction conditions of 397 °C and 10 bar. The liquid reaction products were collected in a container that was immersed in a dry ice bath. After condensation, the products were separated into an organic layer and an aqueous layer. Each layer was injected into a gas chromatography instrument for analysis. The gas phase product, however, was collected in an inverted big bottle via water drain. The collected gas was analysed by gas chromatography as well.

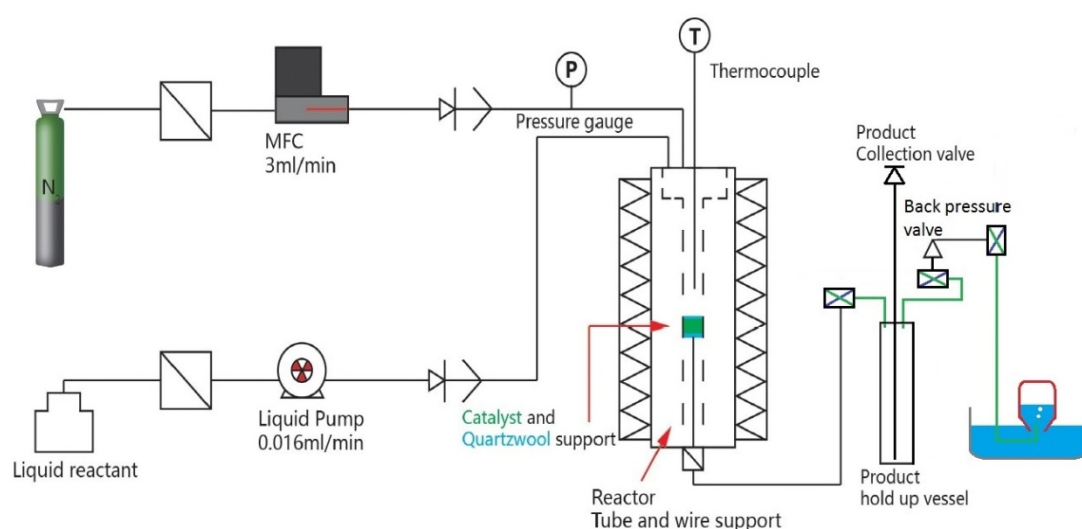


Figure S1 The configuration of the fix bed reactor

## 2. Gas chromatography (GC)

Liquid product:

To both organic layer and aqueous layer products was added 1% 2-Isopropylphenol as an internal standard before injection into an Agilent 7890B GC for analysis. In addition, a relative respond factor to internal standard was added as a parameter to make the calculation more accurate.

The relative response factor can be obtained by injecting the same weight of each known compound and 2-Isopropylphenol. The reciprocal of peak area ratio is equal to their relative respond factor to internal standard.

The weight percentage of each product can be inferred from the formula below:

$$\frac{\text{Product weight percentage}}{1\%} = \left( \frac{\text{Product peak area}}{\text{Internal product peak area}} \right) \times \left( \frac{\text{Internal standard respond factor}}{\text{Product respond factor}} \right)$$

The product produced in weight equal to its weight percentage times the total weight of the liquid collected.

Gas product:

There were two main gas products produced during the catalytic reaction, one was light hydro-carbon, the other was carbon dioxide. An Agilent 7890B GC was used to analyse the concentration of the two groups of gas compound by a flame ionisation (FID) and thermal conductivity (TCD), respectively.

The total volume of the gas product was recorded under normal pressure. Subsequently, the gas was taken out from the bottle by a syringe and injected into the GC for analysis. The total amount of the gas compound produced equal to its concentration multiple the total volume of the gas collected.

A 5% methane in argon mixture gas was used as an external standard to calibrate the concentration of hydrocarbon in the gas collected. The concentration of hydrocarbon produced is equal to the integration of the total peak area on the FID result multiplied by 5% divided by the peak area of the external standard methane. In this case, the calculated concentration assumed that the entire light hydrocarbon was methane. The relative response factor for most of the light hydrocarbon is similar to methane's, hence it was assume that their response factor to FID detector was the same.

In terms of carbon dioxide concentration, a calibration curve (Fig. S2) was made by injecting different concentration of CO<sub>2</sub>. From this curve we can claim that CO<sub>2</sub> concentration in gas product is equal to its integrated peak area divided by 711.

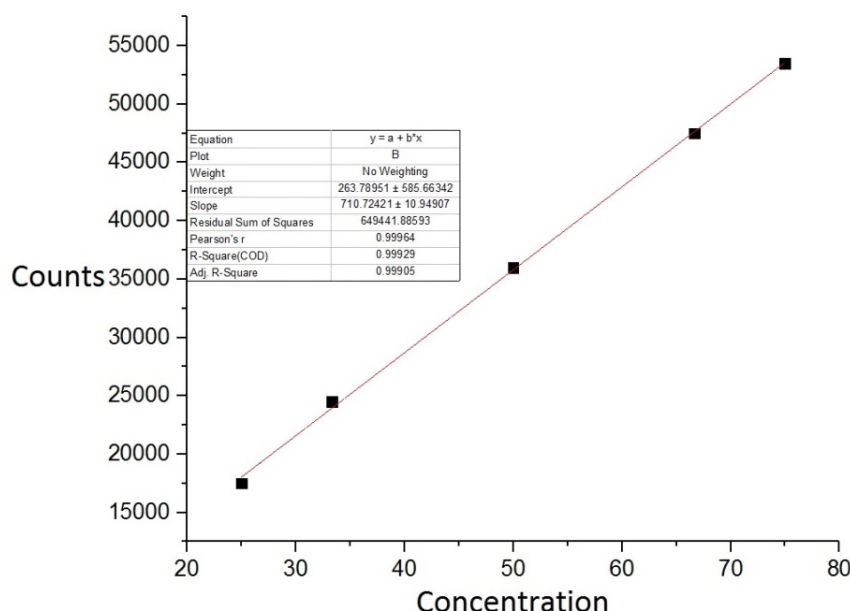


Figure S2 The calibration curve of CO<sub>2</sub> for the TCD detector

### 3. Thermogravimetric analysis

Carbon deposition took place on the active sites in catalyst during the reaction. Thermogravimetric analysis was applied to determine how much coke was formed after the catalytic reaction. The instrument was a SDT Q600 made by TA instrument. As the temperature reached 200°C a significant drop in weight began and continued until 600°C, as shown in Fig. S3. During this temperature range, the coke will be burned out under a steady air flow with 100ml/min. The coke formed during the reaction equal to the weight percentage lost times the total weight of the catalyst after reaction.

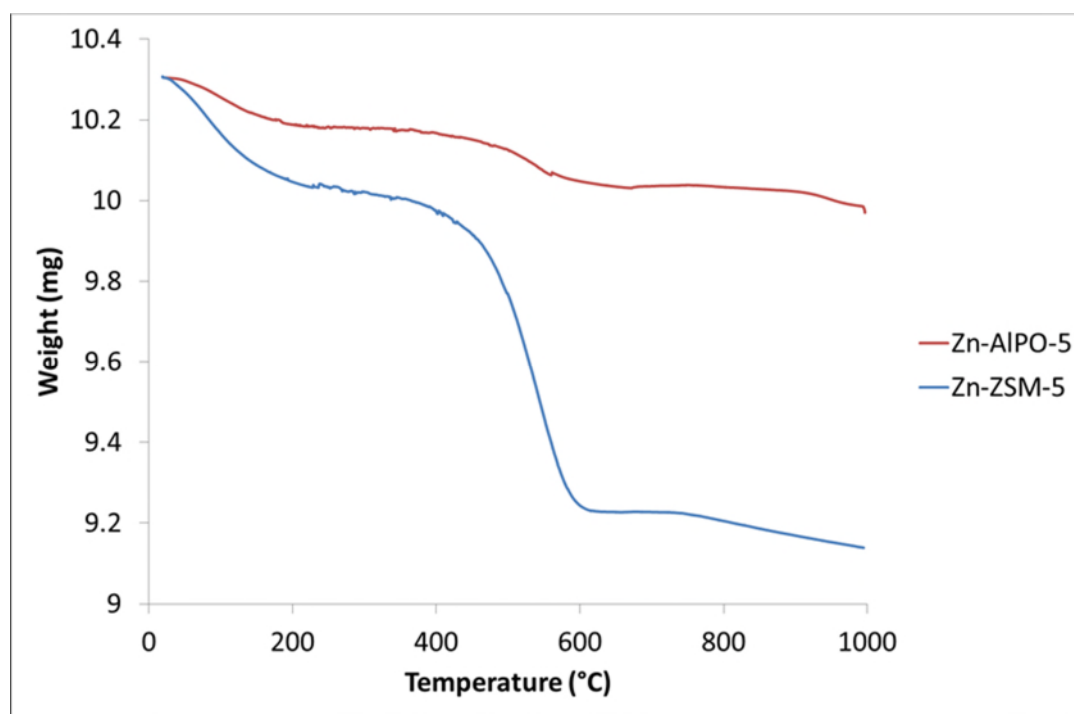


Figure S3 The TGA result for (A) Zn-ZSM-5 and (B) Zn-AlPO-5 after 24 hours catalytic reaction. A significant drop in weight between 200 and 600 °C indicated the ratio of coke formed during the reaction.

It can be seen that the ratio of coke in the Zn-ZSM-5 catalyst is approximately to 8% whereas only 2% for the Zn-AlPO-5. The big difference can be attributed to the nature of acidic sites and stereospecific reactions taken place in the zeolite cavity. For Zn-ZSM-5, all the hydrolysis, decarboxylation (cracking) and aromatisation (condensation) reactions of GVL should have been taken place in the Zn-ZSM-5 cavity while Zn-AlPO-5 only catalysed the hydrolysis reaction of GVL. Thus, the residue carbons from cracking/condensation reactions in Zn-ZSM-5 are apparently higher. Nevertheless, these levels of coke represent very small amount of carbon accumulated in zeolites. Their carbon contributions accounted only 0.7% and 0.2%, respectively after 24 hours of reactions over the two zeolites.”

Table S1 The products produced from each catalyst over 24 hours of catalytic reaction.

Products (mol of carbon produced)	Zn-AlPO-5	AlPO-5	Zn-ZSM-5	ZSM-5
GVL (reactant)	0.160	0.445	0.0160	0.0517
Pentenoic acid	0.182	0.0125	0	0.0283
Carbon dioxide	0.0137	0.0015	0.0620	0.0397
Hydrocarbon	0.0594	0.005	0.142	0.0963
Aromatics	0	0	0.104	0.102

Table S2 The composition of light hydrocarbon in gas phase

Compound	mol %
Methane	3
Ethane	3
Ethylene	1
Propane	8
Propylene	4
Isobutene	6
n-butane	7
1-butene	25
trans-2-butene	19
Isobutene	3
cis-2-butene	18
Isopentane	1

Table S3 The composition of aromatics in oil phase products

Compound	mol %
Benzene	1.7
Toluene	9
Xylene and isomers	20
Alkyl substituted benzene	61
(Alkyl substituted) naphthalene	8

The mass balance calculation:

The total mole of carbon feed to the reactor during the reaction period:

$(\text{GVL solution concentration} \times \text{flow rate} \times \text{reaction time} \times 5 \text{ carbon / GVL molecule}) / (\text{GVL molecule}$

$\text{weight}) = (40\% \times (0.016 \text{ ml/min}) \times (60 \text{ min/h}) \times 24 \text{ h} \times (5 \text{ carbon/mol})) / (100 \text{ g/mol}) = 0.46 \text{ mol}$

In table S1, we can add up all the carbon produced from each compound as well as the formation of coke then divided by 0.46 so that we can obtain the mass balances:

Zn-AlPO-5 90.4%

AlPO-5 100.9%

A similar carbon mass balance of > 90% was reported for Zn-ZSM-5<sup>[1]</sup>

### **The Zn contents in synthesised Zn-ZSM-5 and Zn-AlPO-5**

From the ICP analysis, the Zn-content in Zn-ZSM-5 was determined to be 0.97/unit cell.<sup>[1]</sup>

However, we encountered difficulties in the ICP analyses for Zn-AlPO-5. Their determined Zn: Al ratios were fluctuated presumably due to the total dissolution of these samples was not easily achieved. Besides, we believe that the ICP data cannot also give information whether the detected zinc ion was from the framework or extra-framework. Instead, the quantity of Zn substitution into AlPO-5 can be better inferred from our NMR data. It is noted that NMR estimation of the created acid sites by  $\text{Zn}^{2+}$  incorporation into AlPO structure via quantitative analysis of  $^{31}\text{P}$  NMR signal of TMPO probe molecule in stoichiometry is very accurate as previously presented.<sup>[2]</sup>

According to our synthesis procedure of Zn-AlPO-5 in the supporting information, the ratio between aluminium and zinc precursor was set at 20 (molar ratio). This suggests that 1.2 acid site per unit cell of catalyst if all the  $\text{Zn}^{2+}$  were successfully substituted into AlPO-5. Please see the calculation below:

$$\text{AlPO unit cell molecule weight} \times 5\% = (27 + 31 + 16 \times 4) \times 24 \times 5\% = 1.2 \text{ /unit cell}$$

From the area integration of the TMPO probe ss-nmr signal, we have obtained 0.32mmol/g of TMPO molecule adsorbed on the Zn-AlPO-5 with stoichiometry to each Bronsted acid site created by each mole of  $\text{Zn}^{2+}$ . This is equal to 0.94  $\text{Zn}^{2+}$  per unit cell:

$$0.32\text{mmol/g} \times \text{AlPO molecular weight} = 0.32\text{mmol} \times (27 + 31 + 16 \times 4) \times 24 = 0.94 \text{ /unit cell}$$

Thus, the NMR result indicates that there is nearly 80% of the  $\text{Zn}^{2+}$  successfully incorporated into the AlPO framework.

As seen from the results, the zinc concentration of Zn-ZSM-5 (0.97/unit cell determined by ICP) and Zn-AlPO-5 (0.94/unit cell inferred from NMR analysis) is comparable to each other.

## Characterisation

### 1. Synchrotron X-ray diffraction

High resolution Synchrotron XRD data were collected on Beamline I11, Diamond Light Source, UK. A detailed description of the beamline can be found elsewhere.<sup>[3]</sup> The energy of the incident X-ray beam was set at 15 keV. The wavelength and the 2 $\theta$ -zero point correction were refined using a diffraction pattern obtained from a high quality silicon powder (SRM640c). The physisorbed water in Zn-AlPO-5 was desorbed under vacuum at 400 °C for 2 h. After that the ammonia gas was introduced into the Zn-AlPO-5. The fine Zn-AlPO-5 powder with ammonia adsorbed was loaded in a 0.5 mm borosilicate glass capillary. High resolution XRD data were obtained from the samples using the multi-analyser crystal (MAC) detectors. The patterns were collected in the 2 $\theta$  range 0-150 ° with 0.001° data binning. Each pattern was collected for an hour for good statistics. In total, there were more than 379 hkl reflections measured, of which at least 100 independent hkl reflections were observed. In a crystallographic point of view, the number of structural variables should not exceed the number of hkl reflections in a refinement. In the Rietveld refinements performed in this work, the number of structural parameters has not exceeded 300.

Using the TOPAS software, the diffraction patterns were analysed by Rietveld refinement methods to obtain structural details. The starting coordinates were based on the AlPO-5 zeolite model by Klap et al. for structural refinement. ([https://doi.org/10.1016/S1387-1811\(00\)00161-X](https://doi.org/10.1016/S1387-1811(00)00161-X)) The Thompson-Cox-Hastings pseudo-Voigt peak function<sup>[4]</sup> was applied to describe the diffraction peaks. The scale factor and lattice parameters were allowed to refine for all the diffraction patterns. The refined structural parameters for pattern were the fractional coordinates (x, y, z) and isotropic displacement factors (Beq) for Zn-AlPO-5 and ammonia atoms, and the site occupancy factors (SOF) describing the adsorbed ammonia molecules within the AlPO-5 framework. The quality of the Rietveld refinements of synchrotron XRD data has been assured with a low goodness-of-fit (Gof) factor, a low weighted profile factor (Rwp) and a well-fitted pattern with acceptable temperature factor (Beq) within experimental errors. All the errors of the atom-atom distances were calculated from the square root of the (Xerror)<sup>2</sup>+(Yerror)<sup>2</sup>+(Zerror)<sup>2</sup> multiplied by the measure distances. The crystallographic data and refinement details are summarized in Table S4.

Table S4 Crystallographic data and details of the Zn-AlPO-5 sample after ammonia-adsorbed

Zn-AlPO-5	
Crystal system	Hexagonal
Space group	<i>P6cc</i>
Py per unit cell	0
2 $\theta$ range refinement ( $^{\circ}$ )	3 – 55
Detector	multi-analyser crystal
Number of parameters	45
Number of hkl's	379
Refinement	Rietveld
<i>a</i> ( $\text{\AA}$ )	13.73113(3)
<i>c</i> ( $\text{\AA}$ )	8.39987(3)
<i>V</i> ( $\text{\AA}^3$ )	1371.56(8)
<i>R</i> <sub>wp</sub> / <i>R</i> <sub>p</sub> / <i>R</i> <sub>exp</sub>	5.939/4.276/2.355
Gof $\chi^2$	2.522
Wavelength ( $\text{\AA}$ )	0.825260(2)
2 $\theta$ Zero point	-0.012416(2)



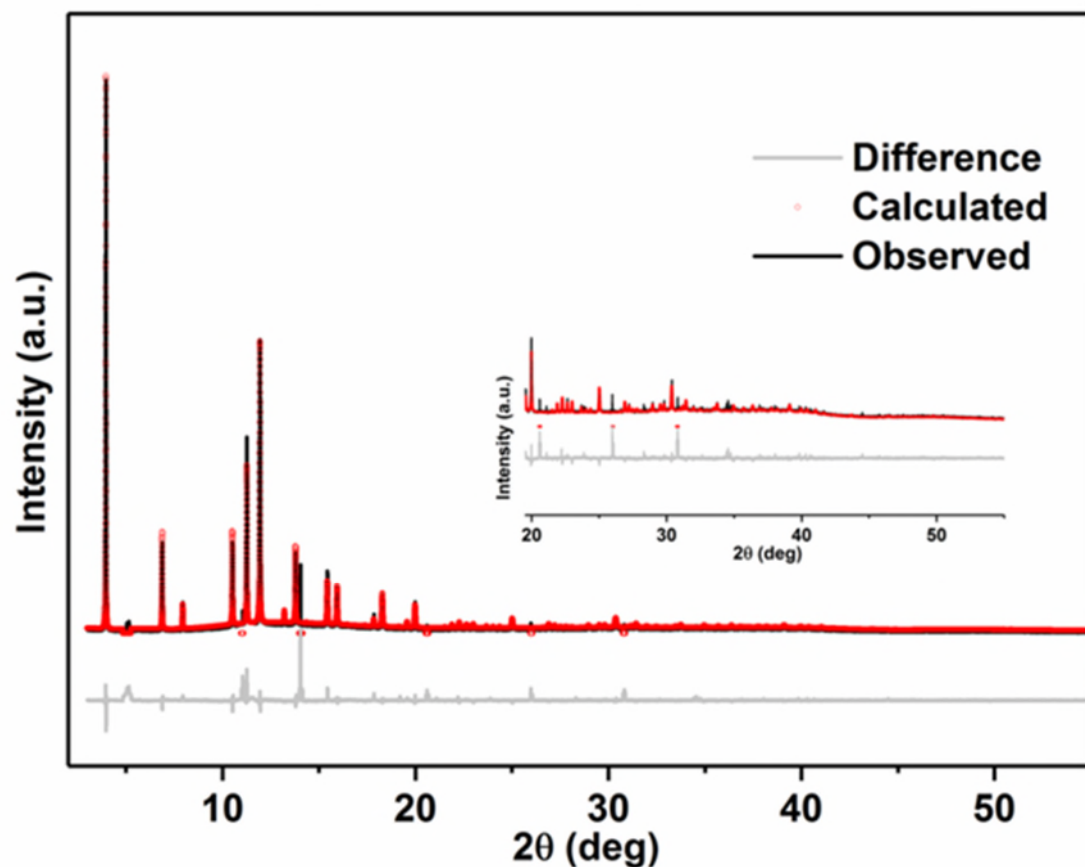


Figure S4. The SXRD data of Zn-AlPO-5 fitted by Rietveld refinement method. The data in the  $2\theta$  range of 2–55° is zoomed in to illustrate the quality of the refinement result. (the peaks 4.85 to 5.25; 10.97 to 11.09; 13.99 to 14.15; 20.54 to 20.68; 25.96 to 26.06; 30.74 to 30.88 were excluded as impurities.)

A Fourier map was generated between the observed and calculated scattering data over the  $2\theta$  range of 2 – 55°. It was used to identify the positions with the highest remaining electron density in the framework, which can indicate the possible positions of the inorganic or organic small molecules (Fig. S5).

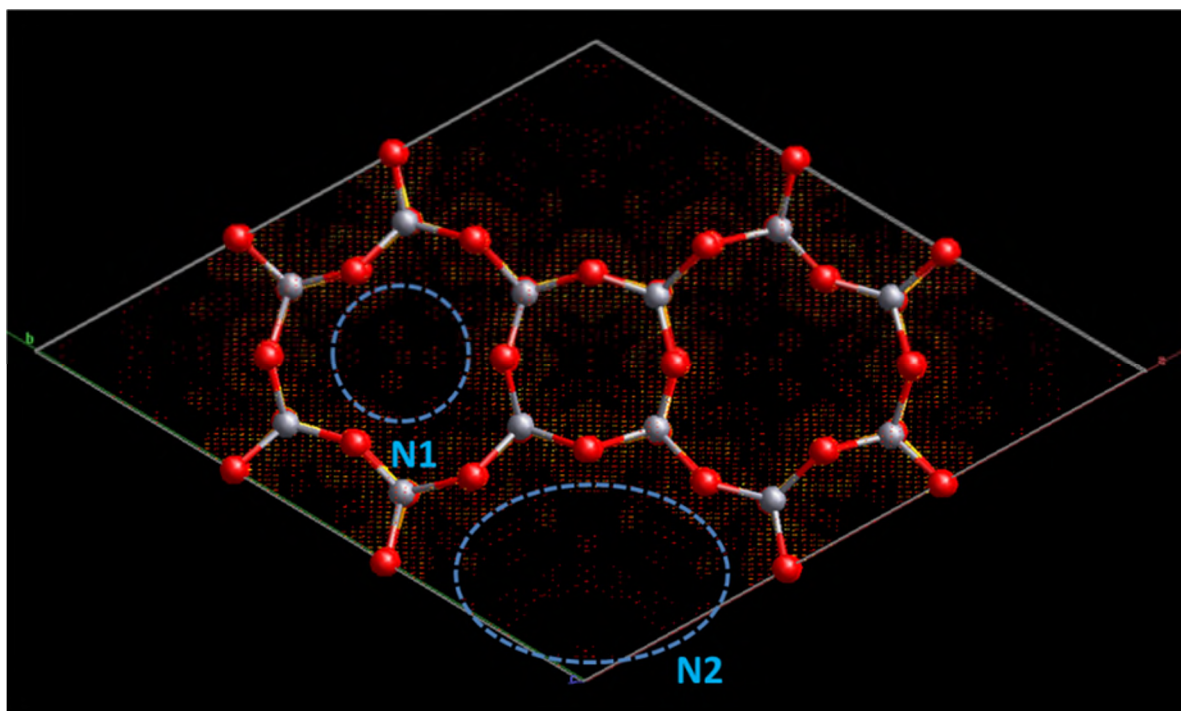


Figure S5. Fourier map of Zn-AlPO-5 with ammonia-adsorbed at room temperature; the blue circles represent the possible electron densities and positions of ammonia molecules.

Table S5. Crystallographic information files from the Rietveld refinement of Zn-AlPO-5 after ammonia-adsorbed

Species	Atom	<i>X</i>	<i>y</i>	<i>z</i>	SOF	<i>B</i> <sub>eq</sub> (Å <sup>2</sup> )	Symmetry multiplicity
Zeolite framework	P	0.45250	0.32952	0.05386	1	5.5(1)	12
	Al	0.45652	0.33599	0.4264	1	2.9(1)	12
	O1	0.4200	0.2069	-0.0026	1	7.4(1)	12
	O2	0.4519	0.3295	0.2246	1	7.4(1)	12
	O3	0.3610	0.3629	-0.0087	1	7.4(1)	12
	O4	0.5737	0.4199	-0.0134	1	7.4(1)	12
Ammonia 1	N1	0.453(9)	2.778(9)	5.274(8)	0.020(1)	16.9(6)	12
Ammonia 2	N2	3.069(5)	1.872(7)	0.335(1)	0.880(1)	15.3(5)	12

## The Rietveld refinement and details of ammonia adsorbed H-ZSM-5 at room temperature.

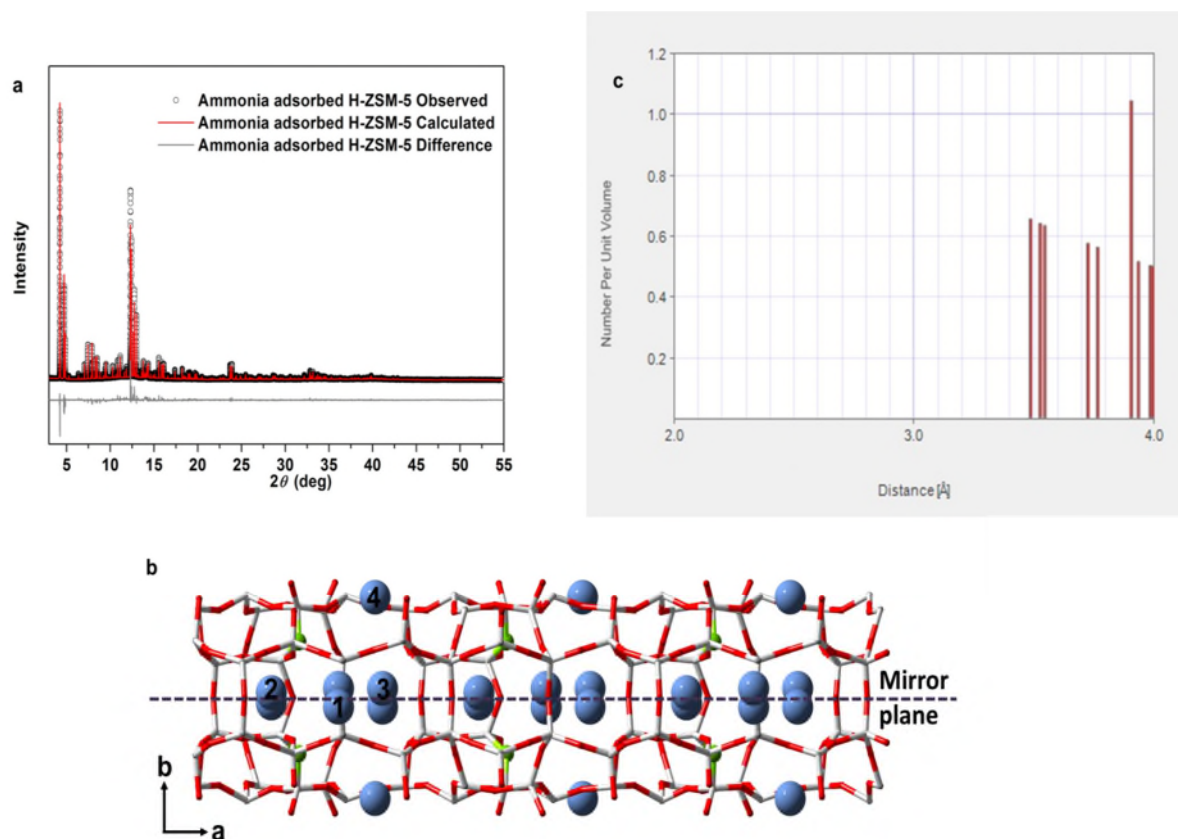


Figure S6. SXR D refinement and the structure of ammonia adsorbed H-ZSM-5 at room temperature. a, Comparison of the experiment data (black circle) and Rietveld refinement (red line) and the difference between them (grey line) for synchrotron PXRD patterns after ammonia adsorbed H-ZSM-5 at room temperature (range from 3 ~ 55°). b, The refined structure of ammonia adsorbed H-ZSM-5 (viewed from c-axis). The framework of H-ZSM-5 is using the stick mode, red stick is O and grey stick is Si. The O18 of Brønsted acid sites are highlighted in green ball and the N of  $\text{NH}_3$  is blue ball. The symmetric ammonia and Brønsted acid sites between mirror plane are illustrated. (dark grape dot line). c, The distribution of N-O<sub>(framework)</sub> distances in range 2.0 to 4.0 Å, which exports from CrystalMaker. There are no peaks below 3.0 Å. Therefore, the closest distance of N-O<sub>(framework)</sub> as  $\text{NH}_4^+$  is 3.486 Å (N-O18).<sup>[5]</sup>

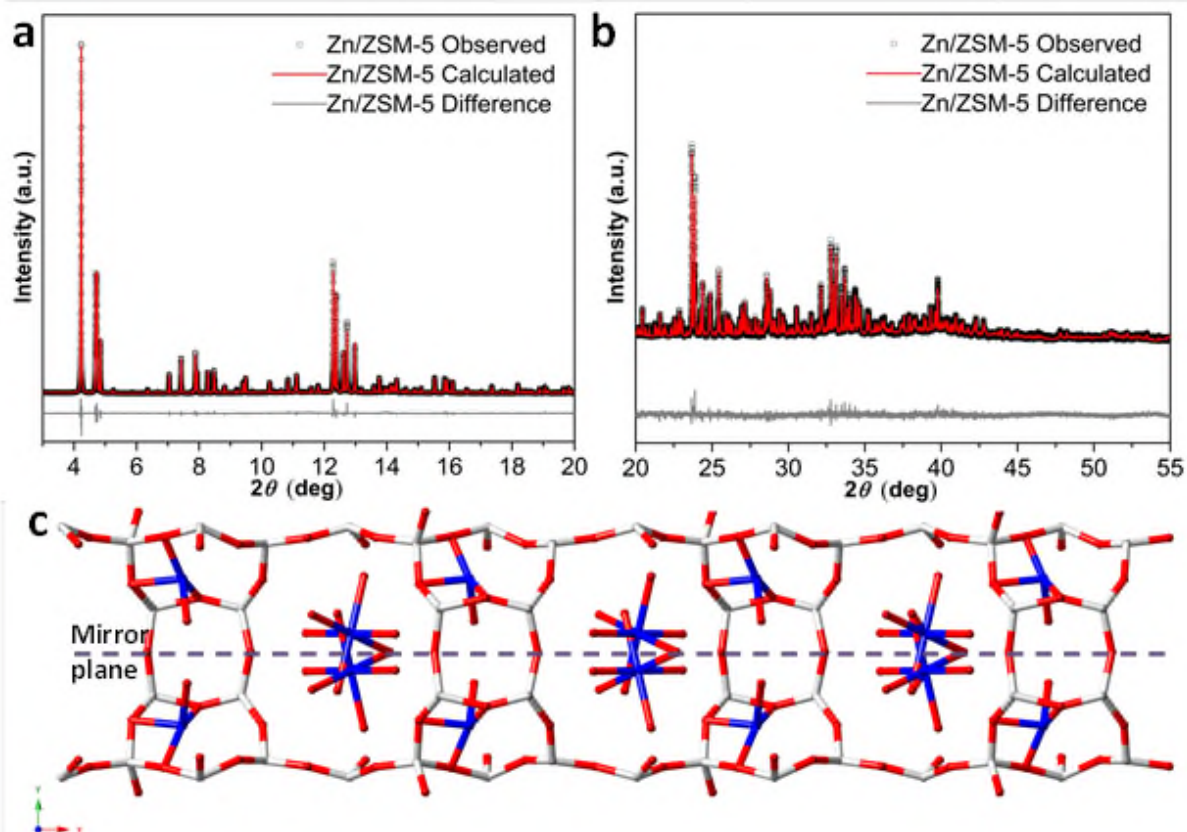


Figure S7. SXRD with the Rietveld refinement and the structure of Zn/ZSM-5 at room temperature. (a) Comparison of the experiment data (black circle) and Rietveld refinement (red line) and the difference between them (grey line) for SXRD patterns of Zn/ZSM-5 at room temperature range from 3 ~ 20° and (b) range from 20 ~ 55°. (c) The refined structure of Zn/ZSM-5 (viewed from z-axis) showing two extra-framework  $\text{Zn}^{2+}$  species were observed, one is surface oxygens immobilized  $\text{Zn}^{2+}$  with terminal Zn-OH as 4 coordinated complex in the cross-channel region and the other one is 6 coordinated  $\text{Zn}^{2+}(\text{H}_2\text{O})_6$  entrapped in the straight channel.<sup>[5]</sup>

## 2. Extended X-Ray absorption fine structure (EXAFS)

The chemical states of Zn and local structures surrounding Zn in the Zn-ALPO sample was probed by using the extended X-ray absorption fine structure (EXAFS) technique. The Zn K-edge EXAFS measurements were performed at beamline BL07A of the Taiwan light source at National Synchrotron Radiation Research Centre in Taiwan. A Si (111) Double Crystal Monochromator (DCM) was used to scan the photon energy. The EXAFS

spectra were measured in the fluorescence mode using a Lytle fluorescence detector for the Zn-ALPO sample. The IFEFFIT software package was used to analyse the EXAFS data to obtain the local structural parameters of Zn. Several constraints were applied to the fitting parameters to exclude unphysical results.

### 3. Ammonia temperature-programmed desorption (NH<sub>3</sub>-TPD)

NH<sub>3</sub>-TPD was performed on Micromeritics AutoChem II 2920. Ca. 0.5 g of the sample was out gassed at 600 °C for 1 h in helium flow followed by NH<sub>3</sub> adsorption at 100 °C for 30 min. Subsequently, the sample was maintained in helium flow at 100 °C for 30 min to remove weakly bound NH<sub>3</sub>. NH<sub>3</sub> desorption was carried out by raising the temperature to 600 °C with a heating rate of 10 °C min<sup>-1</sup>.

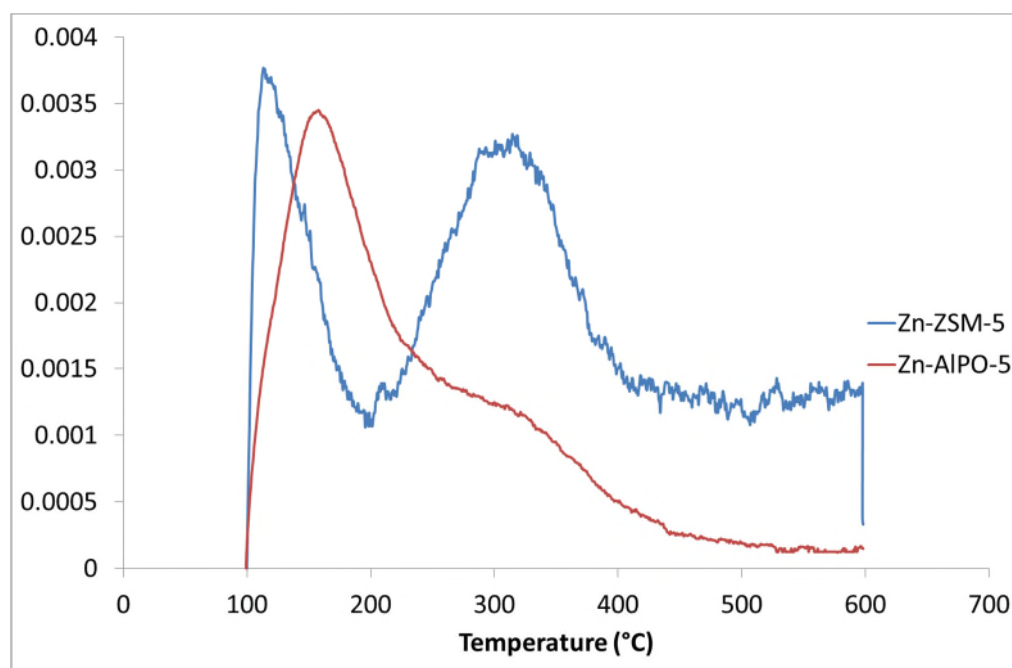


Figure S8 The NH<sub>3</sub>-TPD results for Zn-AlPO-5(red) and Zn-ZSM-5(blue).

### 4. Nuclear magnetic resonance (NMR)

Trimethylphosphine oxide (TMPO)-adsorbed sample was prepared for <sup>31</sup>P MAS NMR. Before loading TMP molecules, about 100 mg of catalysts was placed in a home-made glass tube and activated at 298 K for 2 h under vacuum (10<sup>-1</sup> Pa) to ensure maximum adsorption of TMPO molecules, which was followed by mixing with CH<sub>2</sub>Cl<sub>2</sub> solution containing 0.1 M TMPO under nitrogen and followed by a 1 h ultrasonic treatment (for equilibrium), and then solvent was evacuated completely under vacuum. The sample tube was then sealed for storage and transferred to Bruker 4 mm ZrO<sub>2</sub> rotor with a Kel-F

endcap in a glove box under nitrogen atmosphere before NMR measurement. Solid state magic angle spinning (MAS) NMR experiments were carried out using a Bruker Avance III 400WB spectrometer at room temperature. To remove the effect of proton spins on quantitative  $^{31}\text{P}$  spectra, a strong radio frequency field (B) is usually applied in a pulsed at the resonance frequency of the non-observed abundant spins ( $^1\text{H}$  herein) which contribute to the coupling of both spin species. If B is strong such that spins of  $^1\text{H}$  is flipped rapidly compared with the spin-spin interactions, the interaction is averaged to zero and consequently the excess broadening is zero. The high power decoupling (HPDEC) was thus used for the quantitative  $^{31}\text{P}$  analysis. Considering the long relaxation time of  $^{31}\text{P}$  nuclei in NMR experiment, we used  $30^\circ$  pulse with the width of  $1.20\ \mu\text{s}$ , 15 s delay time. The radiofrequency for decoupling was 59 kHz. The spectral width was 400 ppm, from 200 to  $-200$  ppm. The number of scans was 800 and spinning frequency was 10 kHz. The  $^{31}\text{P}$  chemical shifts were reported relative to 85% aqueous solution of  $\text{H}_3\text{PO}_4$ , with  $\text{NH}_4\text{H}_2\text{PO}_4$  as a secondary standard (0.81 ppm). The quantitative analysis of adsorbed TMPO molecules was then calculated according to the calibration line established by running standard samples with various adsorbed TMPO concentration.

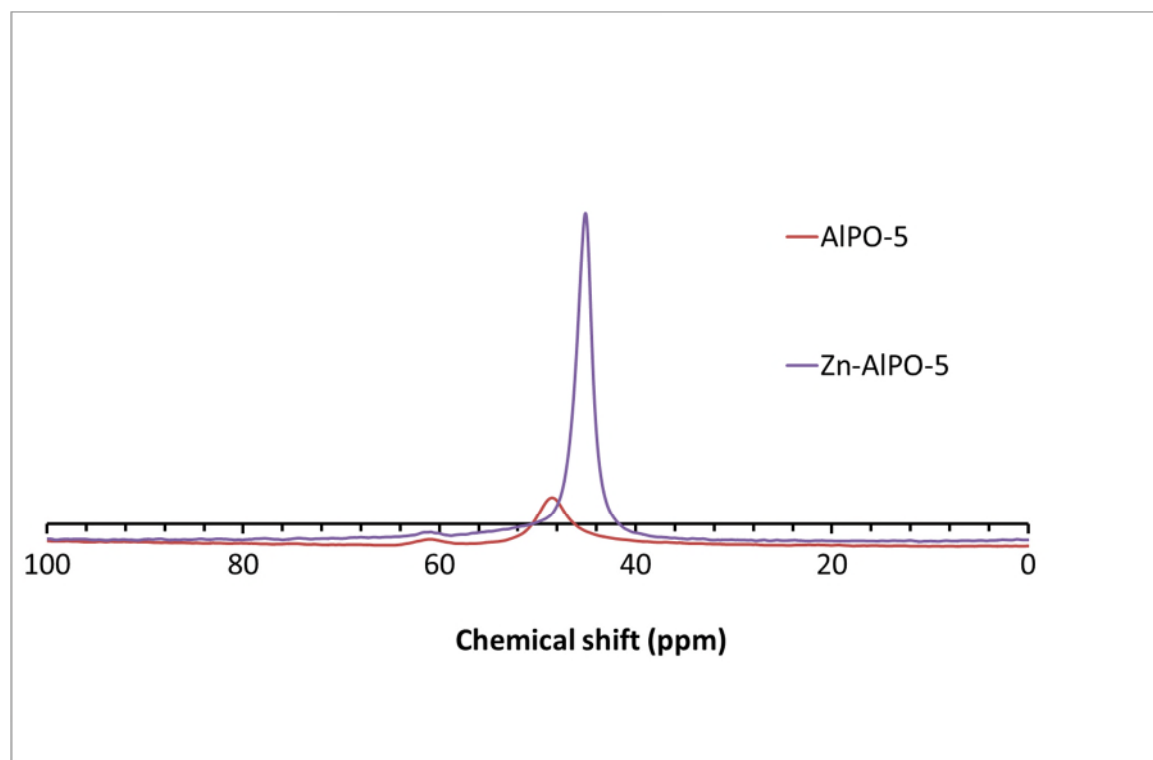


Figure S9  $^{31}\text{P}$  NMR of TMPO adsorbed Zn-AlPO-5/AlPO-5

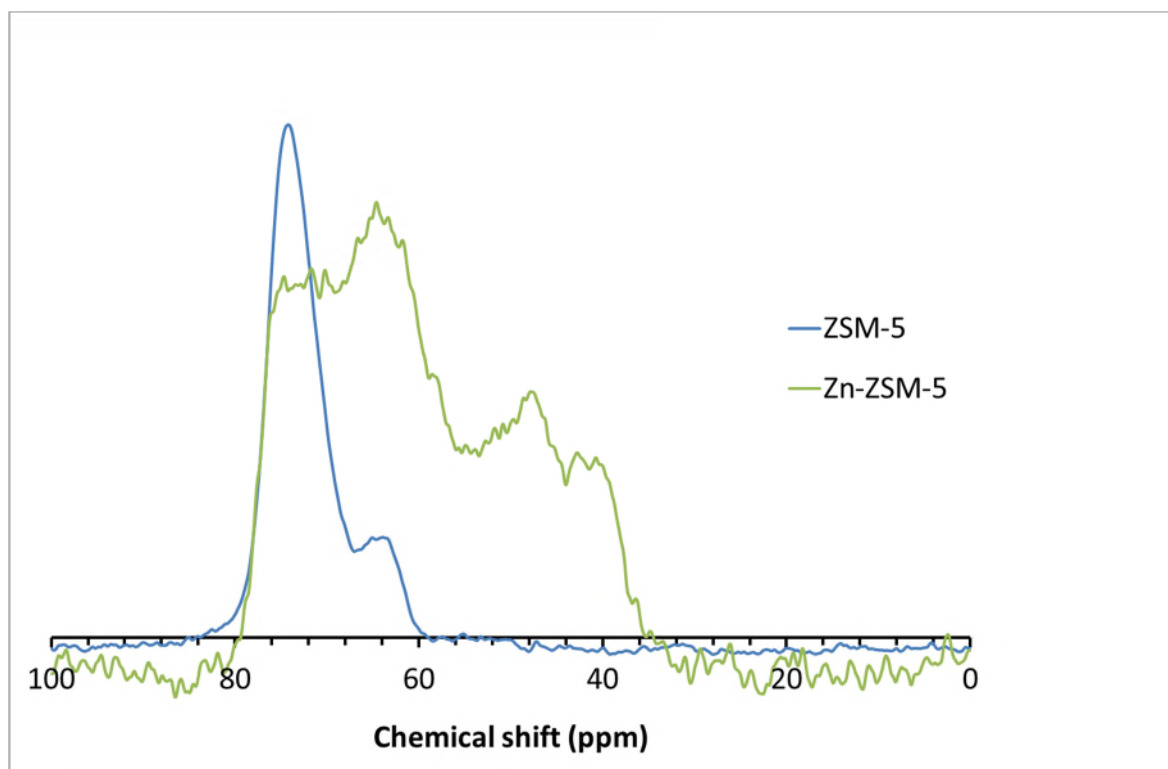


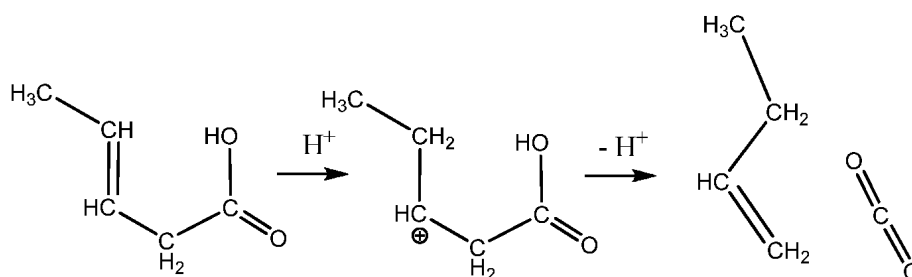
Figure S10  $^{31}\text{P}$  NMR of TMPO adsorbed Zn-ZSM-5/ZSM-5

The integration of the TMPO probe NMR indicated 0.32mmol/g of TMPO molecule adsorbed. This result inferred 0.32mmol/g of zinc ion substituted in the framework creating the weak Brønsted acid site.

The synthesis process of Zn-AlPO-5 was implemented with the ratio between aluminium and zinc precursor was 20 (molar ratio). This indicated approximately 0.41 mmol acid site per gram of catalyst if all the substitution successfully done. Please see the calculation below:

$$\frac{1\text{g} \times \text{mole percentage of zinc loading}}{\text{AlPO}_4 \text{ molecule weight}} = \frac{1 \times 5\%}{27+31+16 \times 4} = 0.41 \text{ mmol}$$

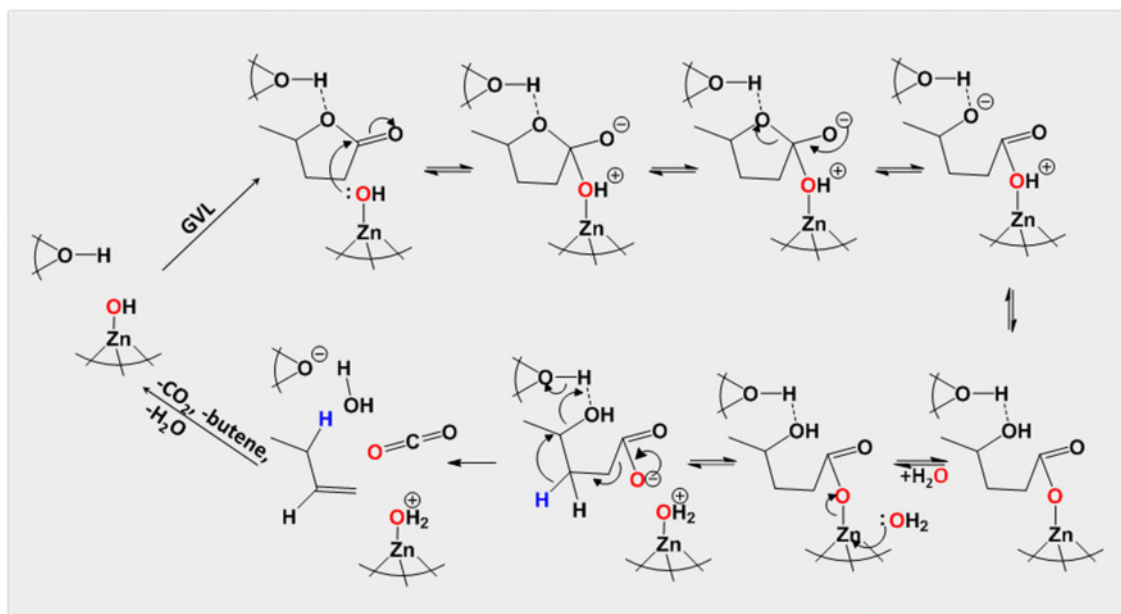
The ratio between the NMR result and the theoretical amount from the calculation indicates approximately 80% of zinc successfully loading into the Zn-AlPO-5 framework.



**Scheme S1:** Strong Brønsted Acid catalysed conversion of GVL to 1-butene and  $\text{CO}_2$



Brønsted Acid site can first catalyse ring opening of GVL to PA, but will subject to subsequent acid-catalyse decarboxylation to form 1-butene and CO<sub>2</sub> rapidly, as shown in the above mechanism in Scheme S1.<sup>[1]</sup>



**Scheme S2.** The proposed mechanism for aromatics/hydrocarbons production from cooperative ring opening hydrolytic decarboxylation of gamma-valerolactone (GVL) with water molecule activation over Zn/ZSM-5 due to the nature of nucleophilic terminal Zn-OH

The proposed mechanism for aromatics production from cooperative ring opening hydrolytic decarboxylation of gamma-valerolactone (GVL) with water molecule activation over Zn/ZSM-5 by regenerative Zn-OH and Brønsted acid site to CO<sub>2</sub> and 1-butene where the latter can further undergo aromatization in the ZSM-5 cage. This route is different from the Brønsted Acid catalysed conversion of GVL to 1-butene and CO<sub>2</sub> described in Scheme S1.



## Effects of Acid Site Concentration and Acid Site Strength

The mild hydrolysis reaction with decarboxylation is likely to be endothermic and slightly entropically favourable at elevated temperature. On the other hand, the direct acid hydrolysis of GVL to butene/ $\text{CO}_2$  is thought to be irreversible and favoured under all relevant reaction conditions. These conclusions are supported by some extensive works on the corresponding mechanistic studies over  $\text{SiO}_2/\text{Al}_2\text{O}_3$  carried out by Dumesic and co-workers. They have also provided some very useful thermodynamic data for the conversions with and without decarboxylation.<sup>[6-7]</sup>

Here we have found our observed hydrolysis of GVL to pentenoic acid at high yield and high selectivity over Zn-AlPO (mild acid strength) as compared to Zn-ZSM-5 (strong acidic strength) without much decarboxylation under comparable residence time and reaction conditions. One main concern is that this impressive result may not be due to their difference in acid strength over these two materials but may be due to the difference in their total acid content that is in contact.

Although collecting detailed residence time studies at long range over these zeolites are important, it is rather difficult to carry out reliable studies over the zeolite based catalysts since unlike typical powder catalysts, they are dominated by a slow diffusion kinetic to the internal pores. But, with reference to the short residence time used by Dumesic and co-workers over  $\text{SiO}_2/\text{Al}_2\text{O}_3$  (similar strong acidic as ZSM-5) a good selectivity to pentenoic acid (49%) can indeed be seen at 648K.<sup>[6]</sup> They later showed that the pentenoic acid is a facile intermediate, which can be converted to butene/ $\text{CO}_2$  at longer residence times or at higher temperatures over their strong acidic powder.<sup>[7]</sup> Using a simple kinetic model they concluded that two parallel routes either for direct GVL decarboxylation to butene/ $\text{CO}_2$  or via petenoic acid over  $\text{SiO}_2/\text{Al}_2\text{O}_3$  are present.<sup>[8]</sup>

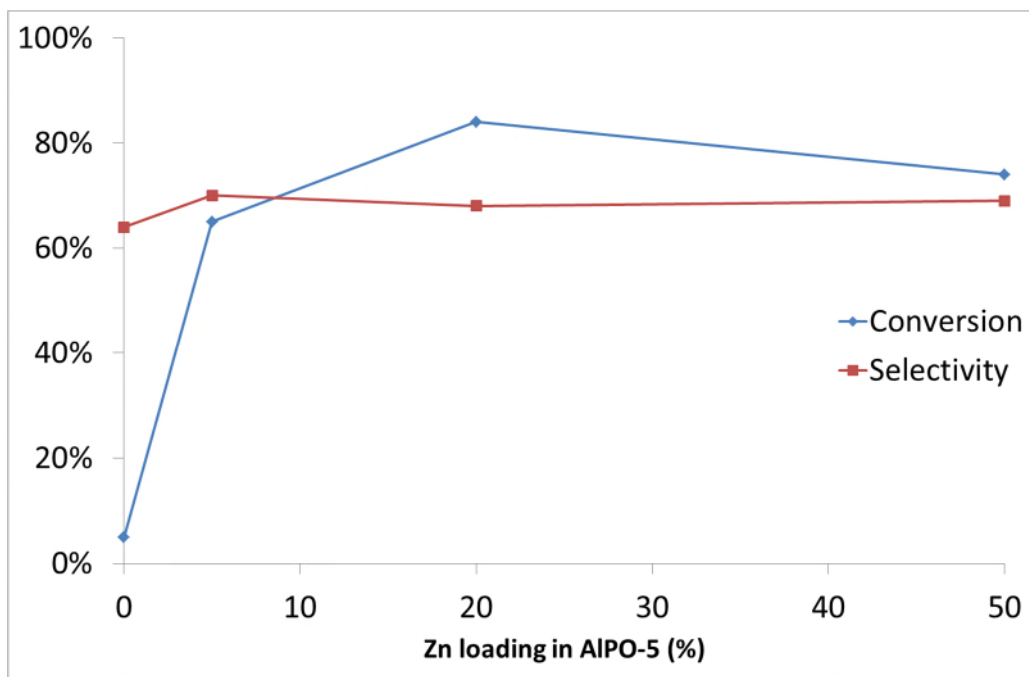


Figure S11 Effect of Zn loading in AlPO-5

It is important for us to find out whether our produced petenoic acid is also sensitive when a longer contact time with acid sites is used under this mild acidic catalyst.

Here, from the above figure (Fig. S11), we have varied the zinc loadings into AlPO-5 by keeping the same residence time of substrate flow. 5%  $\text{Zn}^{2+}$  corresponds to the Bronsted acid site concentration of ca. 1.0 mmol/g; 20%  $\text{Zn}^{2+}$  to ca. 4.0 mmol/g (the same acid concentration as our pure ZSM-5) and 50%  $\text{Zn}^{2+}$  to ca. 10.0 mmol/g, etc. Interestingly, the conversion and selectivity (70%) do not seem to change much according to the increasing acid content in our case. It looks only a small quantity of Zn-AlPO is sufficient to achieve the thermodynamic equilibrium. Clearly, unlikely the previous studies over  $\text{SiO}_2/\text{Al}_2\text{O}_3$ , the presence of excess ‘weak acid sites’ this time, does not seem to lead to any detrimental effect to attenuate the selectivity (or yield). Notice that only 10% selectivity to pentenoic acid is obtained over the pure SZM-5 which contains the same acid content (but stronger acid strength). We believe the use of high density but weaker acid sites in Zn-AlPO-5 (corresponding to 45 ppm  $^{31}\text{P}$ -TMPO) can render the conversion of GVL to high yield and high selectivity towards pentenoic acid without much decarboxylation over the Zn-AlPO-5 sample. It is noted that this above preliminary account should be further supported by more extensive investigations into the corresponding reaction mechanisms in future.

At present, the PA selectivity of 70% only looks moderate from a general catalysis view. However, as stated, the mild hydrolysis reaction with decarboxylation reaction of GVL, which are endothermic and slightly entropically favourable at elevated temperature (marginally temperature effect is expected) hence the PA yield is likely to be equilibrium limited. In Figure S11, we used different loadings of Zn-AlPO-5 for the conversion of GVL to PA. The conversion and selectivity (70%) do not seem to change much according to the increasing acid content in our case. Without the calculation of the thermodynamic equilibrium (no data are not available in database), it looks only a small quantity of Zn-AlPO is sufficient to achieve the likely thermodynamic equilibrium position of this reaction route. It may therefore be difficult to breach over this selectivity/conversion by developing other new catalysts.

### **Nature of weak acid sites**

It is known that hydrolysis of GVL can be catalysed by both Lewis or Bronsted acid sites of the zeolite catalysts. Lewis acid site can be converted to Bronsted acid site upon the adsorption with water molecule, for example. It is known that ZnO can give terminal Zn-OH groups in the presence of water.

As widely reported in literature, the terminal Zn-OH in Zn-ZSM-5 not only possesses acidity property but can catalyse nucleophilic attack to lactone group, leading to decarboxylation reaction of GVL. However, we do not see any significant decarboxylation activity of GVL when Zn-AlPO-5 is used (pentenoic acid is produced instead). This contrasts to the expectation that ZnO if existed in this sample is envisaged to cover with Zn-OH in the presence of GVL/water feed to account for the insignificance of the dehydroxylation activity.

Since we have shown in the main manuscript that ammonia titration cannot provide a good resolution of Bronsted and Lewis acidity in materials. However, the TMPO/SSNMR method for acid site titration is more accurate as shown in literature,<sup>[9]</sup> which indicates the weak Bronsted acid sites present in our sample (45 ppm). Although Lewis sites show shifts in a similar range to that of the "weak BAS sites" but the reported value is actually around 55ppm.

Here, we attribute the creation of weak Bronsted acid sites by the Zn<sup>2+</sup> substitution to AlPO structure to the mild hydrolysis activity of GVL without decarboxylation. However, we still

cannot exclude the possibility of any minor Zn containing phase with water-tolerant Lewis sites to be responsible for such mild hydrolytic catalysis.

However, AlPO is built upon oxygens interconnections with equal molar  $\text{Al}^{3+}$  and  $\text{P}^{5+}$  as pseudo tetra-valent elements ( $\text{M}^{4+}$ , such as  $\text{Si}^{4+}$ ) in zeolitic structure with overall charge neutrality. As similar to the mechanism for the creation of Bronsted acid in aluminosilicate zeolite via the substitution of  $\text{Si}^{4+}$  by  $\text{Al}^{3+}$ , any metal cations (e.g.  $\text{Na}^+$ ,  $\text{K}^+$ ,  $\text{H}^+$  and so on) present in the synthesis mixture will be adsorbed on the internal surface to compensate the corresponding negative charge of the framework. Thus, to obtain the proton-form zeolite, ammonium nitrate is used to exchange the metal cations and followed by calcination. Similarly, during the AlPO synthesis, the incorporated  $\text{Zn}^{2+}$  may have substituted  $\text{Al}^{3+}$  (no extra-framework  $\text{Zn}^{2+}$  species were found), resulting in a similar charge unbalance hence creating a corresponding Bronsted acid proton in the final sample after pre-treatments. Further information on the mechanism for the creation of Bronsted acid site in AlPO could be found in the reference.<sup>[10]</sup>

### Catalyst Stability:

In terms of the catalyst stability, Zn-AlPO-5 has been evaluated at 12 hours, 24 hours and 48 hours, respectively, see Fig. S12. The yield of pentenoic acid appeared to be very stable and with no significant deactivation. In addition, the coke formed after 24 hours of reaction was less than 0.2% of the total carbon indicating the catalyst was still in very good condition.

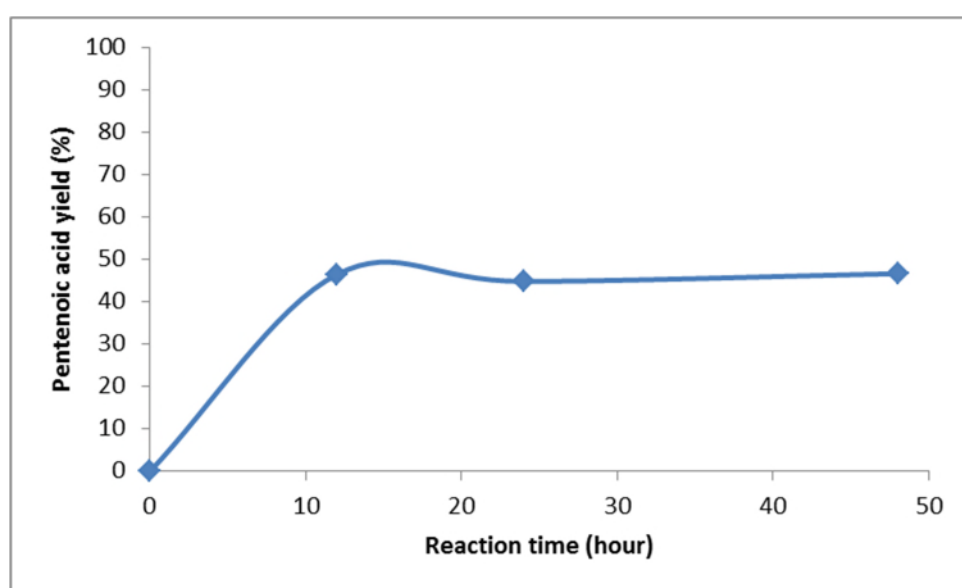


Figure S12 Pentenoic acid yield (%) analysed at 0, 12, 24 and 48 hours.

## References

- [1] L. Ye, Q. Song, B. T. W. Lo, J. L. Zheng, D. J. Kong, C. A. Murray, C. C. Tang, S. C. E. Tsang, *Angew. Chem. Int. Ed.* **2017**, *56*, 10711-10716.
- [2] Y. K. Peng, Y. C. Hu, H. L. Chou, Y. Y. Fu, I. F. Teixeira, L. Zhang, H. Y. He, S. C. E. Tsang, *Nature Comm.* **2017**, *8*.
- [3] S. P. Thompson, J. E. Parker, J. Potter, T. P. Hill, A. Birt, T. M. Cobb, F. Yuan, C. C. Tang, *Review of Scientific Instruments* **2009**, *80*.
- [4] P. Thompson, D. E. Cox, J. B. Hastings, *Journal of Applied Crystallography* **1987**, *20*, 79-83.
- [5] L. Ye, B. T. W. Lo, J. Qu, I. Wilkinson, T. Hughes, C. A. Murray, C. C. Tang, S. C. E. Tsang, *Chem. Commun.* **2016**, *52*, 3422-3425.
- [6] J. Q. Bond, D. M. Alonso, D. Wang, R. M. West, J. A. Dumesic, *Science* **2010**, *327*, 1110-1114.
- [7] J. Q. Bond, D. M. Alonso, R. M. West, J. A. Dumesic, *Langmuir* **2010**, *26*, 16291-16298.
- [8] J. Q. Bond, D. Wang, D. M. Alonso, J. A. Dumesic, *Journal of Catalysis* **2011**, *281*, 290-299.
- [9] A. M. Zheng, S. B. Liu, F. Deng, *Chem. Rev.* **2017**, *117*, 12475-12531.
- [10] B. M. Weckhuysen, R. R. Rao, J. A. Martens, R. A. Schoonheydt, *European Journal of Inorganic Chemistry* **1999**, 565-577.